Chinese Journal of Polymer Science Vol. 31, No. 6, (2013), 924–937

Chinese Journal of Polymer Science

DRUG AND PLASMID DNA CO-DELIVERY NANOCARRIERS BASED ON ABC-TYPE POLYPEPTIDE HYBRID MIKTOARM STAR COPOLYMERS*

Tao Liu, Yan-feng Zhang and Shi-yong Liu**

CAS Key Laboratory of Soft Matter Chemistry, Department of Polymer Science and Engineering, University of Science and Technology of China, Hefei 230026, China

Abstract We report on the fabrication of self-assembled micelles from ABC-type miktoarm star polypeptide hybrid copolymers consisting of poly(ethylene oxide), poly(L-lysine), and poly(ε-caprolactone) arms, PEO(-*b*-PLL)-*b*-PCL, and their functional applications as co-delivery nanocarriers of chemotherapeutic drugs and plasmid DNA. Miktoarm star copolymer precursors, PEO(-*b*-PZLL)-*b*-PCL, were synthesized at first *via* the combination of consecutive "click" reactions and ring-opening polymerizations (ROP), where PZLL is poly(ε-benzyloxycarbonyl-L-lysine). Subsequently, the deprotection of PZLL arm afforded amphiphilic miktoarm star copolymers, PEO(-*b*-PLL)-*b*-PCL. In aqueous media at pH 7.4, PEO(-*b*-PLL)-*b*-PCL self-assembles into micelles consisting of PCL cores and hydrophilic PEO/PLL hybrid coronas. The hydrophobic micellar cores can effectively encapsulate model hydrophobic anticancer drug, paclitaxel; whereas positively charged PLL arms within mixed micellar corona are capable of forming electrostatic polyplexes with negatively charged plasmid DNA (pDNA) at N/P ratios higher than *ca*. 2. Thus, PEO(-*b*-PLL)-*b*-PCL micelles can act as co-delivery nanovehicles for both chemotherapeutic drugs and genes. Furthermore, polyplexes of pDNA with paclitaxel-loaded PEO(-*b*-PLL)-*b*-PCL micelles exhibited improved transfection efficiency compared to that of pDNA/blank micelles. We expect that the reported strategy of varying chain topologies for the fabrication of co-delivery polymeric nanocarriers can be further applied to integrate with other advantageous functions such as targeting, imaging, and diagnostics.

Keywords: Miktoarm star copolymers; Gene delivery; Co-delivery; Polypeptide; Self-assembly.

Electronic Supplementary Material Supplementary material is available in the online version of this article at http//dx.doi.org/10.1007/s10118-013-1281-0.

INTRODUCTION

Due to their unique physicochemical properties such as biocompatibility and degradability, polypeptide-containing hybrid block copolymers have emerged to be the recent research focus[1–3]. Polypeptide chains can undergo reversible transition from random coils to α-helix or β-sheet secondary conformations under proper external stimuli such as pH, ionic strength, and temperature, which is also accompanied with dramatic changes in water solubility[4, 5]. Thus, the integration of polypeptide segments endows conventional synthetic block copolymers with more complex and intriguing hierarchical self-assembling nanostructures in both solution and bulk states[6–8].

* The work was financially supported by the National Natural Science Foundation of China (Nos. 21274137, 91027026 and 51033005), Fundamental Research Funds for the Central Universities, and Specialized Research Fund for the Doctoral Program of Higher Education (SRFDP, 20123402130010).
** Corresponding author: Shi-yong Liu (刘世勇), E-mail: sliu@ustc.edu.cn
Invited paper dedicated to Professor Fosong Wang on the occasion of his 80th birthday
Received January 7, 2013; Revised February 5, 2013; Accepted February 15, 2013
doi: 10.1007/s10118-013-1281-0

Previous literature reports in this field have focused on the synthesis and supramolecular self-assembly of amphiphilic polypeptide hybrid block copolymers of linear chain topology[9, 10]. In this context, extensive investigations have been conducted by Lecommandoux, Klok, Schlaad, and Deming research groups[11–16]. A variety of amphiphilic polypeptide hybrid diblock copolymers consisting of hydrophobic blocks such as polybutadiene (PB), polyisoprene (PI), polystyrene (PS), or poly(ε-caprolactone) (PCL) and hydrophilic ones such as poly(L-glutamic acid) (PLGA) or poly(L-lysine) (PLL). Chen *et al*.[17, 18] also reported the synthesis of peptide hybrid ABC or ABA linear triblock copolymers and their self-assembling behavior in aqueous solution. In addition, polypeptide-based double hydrophilic block copolymers (DHBCs) were also synthesized[19–22]. Lecommandoux and Deming research groups previously reported the synthesis and vesicle formation/inversion of purely polypeptide diblock copolymers[23, 24]. Zhang *et al*. and our research group previously reported the pH- and thermo-responsive self-assembling behavior of poly(*N*-isopropylacrylamide)-*b*-poly(L-glutamic acid), PNIPAM-*b*-PLGA, in aqueous media[25, 26].

It should be noted that all the above examples deal with linear polypeptide hybrid block copolymers. On the other hand, it is well-known that chain architectures of block copolymers can dramatically affect their supramolecular self-assembling nanostructures and corresponding functions[27]. Compared to conventional synthetic block copolymers, the chain topology and hierarchical secondary structure formation of polypeptide sequences of polypeptide hybrid block copolymers of non-linear chain topology are expected to add extra complexity to their self-assembling characteristics[28]. Kim and coworkers[29] recently reported the synthesis of three-arm star block copolymers consisting of PS and poly(γ-benzyl-L-glutamate) (PBLG) sequences *via* a combination of atom transfer radical polymerization (ATRP) and ring-opening polymerization (ROP). Recently, Lecommandoux *et al*.[30] synthesized Y-shaped miktoarm star block copolymers, PS-*b*-$(PLGA)_2$, and investigated their self-assembly in aqueous media. We previously reported the synthesis of AB_2 Y-shaped star polypeptide copolymers, PLL-*b*-$(PLGA)_2$, by combining ROP and click reaction techniques and investigated the pH-responsive self-assembly in aqueous solution[31].

When more than two types of chain segments are arranged in a nonlinear fashion, the simplest form would be ABC miktoarm star copolymers. Note that their supramolecular hierarchical self-assembly in selective solvents have been investigated by Lodge, Hillmyer, and coworkers[32–34]. It is worthy of noting that the synthesis and self-assembly of ABC-type polypeptide hybrid miktoarm star copolymers have been less explored; in addition, more research efforts need to be input in terms of their functional applications. Amphiphilic miktoarm star copolymers are known to self-assemble into core-shell type micellar nanoparticles and can be utilized as nanocarriers of hydrophobic chemotherapeutic drugs[31, 35, 36]. We envisage that if positively charged polypeptides such as PLL were employed as the corona-forming block, self-assembled micelles should also be capable of acting as delivery nanovehicles of plasmid DNA (pDNA)[37–40]. Thus, co-delivery of drugs and genes might be achieved based on non-linear shaped polypeptide hybrid block copolymers. Recently, the strategy of drug and gene co-delivery by the same nanocarrier has been developed as a new direction in cancer therapy to synergistically overcome chemotherapy-related issues such as multidrug resistance (MDR)[41–45]. For example, Yang and co-workers[46] originally reported an elegant example based on hydrophobically modified cationic copolymers, the self-assembled nanoparticles of which can effectively encapsulate hydrophobic anticancer drugs and form electrostatic polyplexes with pDNA together. *In vitro* gene transfection and subsequent *in vivo* experiments revealed synergistic cancer therapeutic effects.

In 2007, Bae and coworkers[47] reported the preparation of micelles from poly(ethylene imine)-*g*-poly(ε-caprolactone), PEI-*g*-PCL, and utilized them as dual nanovehicles of anticancer drug doxorubicin and pDNA. Preliminary in vitro cell experiments based on HepG2 cells demonstrated that the encapsulation of anticancer drug imposed certain effects on the transfection efficiency, exhibiting a promising potential as a composite nanovehicle to overcome MDR. Dong and co-workers[42, 48] fabricated amphiphilic graft copolymers, PCL-*g*-PDMA, where PDMA is poly[(2-dimethylamino)ethyl methacrylate], and employed the resultant cationic micelles for the co-delivery of drug paclitaxel and pDNA, aiming to achieve combinatorial therapy. Based on these results, the authors further developed amphiphilic PEO-*b*-PCL-*b*-PDMA triblock copolymer for the co-

delivery of paclitaxel and pDNA. Similarly, Wang and co-workers[44] reported a "two-in-one" micelleplex based on triblock copolymers, PEO-*b*-PCL-*b*-poly(2-aminoethyl ethylene phosphate) (PEG-*b*-PCL-*b*-PPEEA). The triblock copolymer-based micelles were employed to encapsulate paclitaxel and complex with siRNA, and the synergistic tumor suppression effect was investigated in detail.

Herein, we report on the fabrication of self-assembled micelles from ABC-type miktoarm star polypeptide hybrid copolymers consisting of poly(ethylene oxide), poly(L-lysine), and poly(ε-caprolactone) arms, PEO(-*b*-PLL)-*b*-PCL, and their functional applications as co-delivery nanocarriers of chemotherapeutic drugs and plasmid DNA (Schemes 1 and 2). Miktoarm star copolymer precursors, PEO(-*b*-PZLL)-*b*-PCL, were synthesized at first *via* the combination of consecutive "click" reactions and ring-opening polymerizations (ROP), where PZLL is poly(ε-benzyloxycarbonyl-L-lysine). Subsequently, the deprotection of PZLL arm afforded amphiphilic miktoarm star copolymers, PEO(-*b*-PLL)-*b*-PCL. It is well-known that PEO, PLL, and PCL segments are biocompatible and/or biodegradable. After characterizing the self-assembled micellar nanoparticles by transmission electron microscopy (TEM) and dynamic light scattering (DLS) techniques, we further explored the capability of PEO(-*b*-PLL)-*b*-PCL micelles as co-delivery nanocarriers of chemotherapeutic drugs and pDNA. MTT cytotoxicity and gel retardation assays, in vitro drug release profile and gene transfection efficiencies were measured for either blank or drug-loaded PEO(-*b*-PLL)-*b*-PCL micelles.

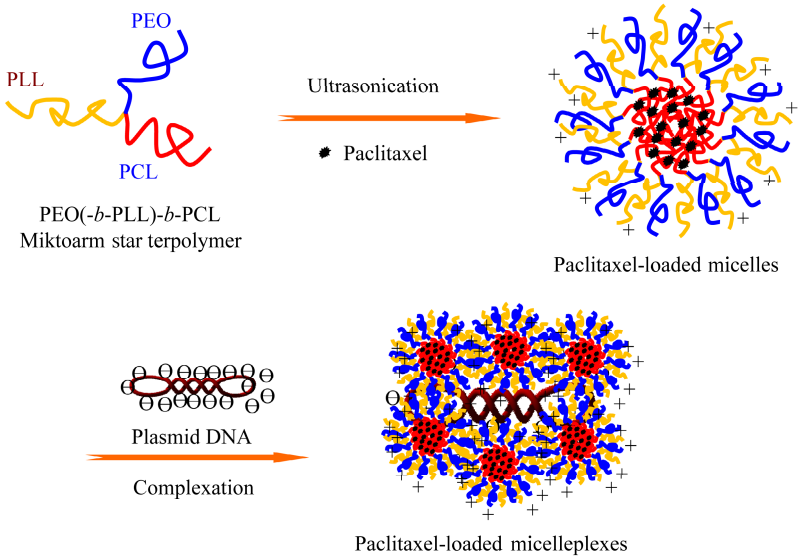

Scheme 1 Schematic illustration for the fabrication of micellar nanoparticles based on ABC-type miktoarm star polypeptide hybrid copolymers, PEO(-*b*-PLL)-*b*-PCL. The obtained polymeric micelles possess hydrophilic coronas of mixed PEO and PLL arms, which were utilized as nanocarriers for the co-delivery of chemotherapeutic drugs and plasmid DNA (pDNA).

EXPERIMENTAL

Materials

Poly(ethylene glycol) monomethyl ether (PEG_{113}-OH, M_n = 5.0 kDa, M_w/M_n = 1.06, mean degree of polymerization, DP, is 113) was purchased from Aldrich and used as received. ε-Caprolactone (ε-CL, 99%, Acros) was vacuum-distilled from CaH_2 just prior to use. *N,N,N′,N″,N″*-pentamethyldiethylene triamine (PMDETA), copper(I) bromide (CuBr, 98%), tin(II) 2-ethylhexanoate ($Sn(Oct)_2$, 95%), anhydrous *N,N*-dimethylformamide (DMF), paclitaxel, and Wang resin (1.47 mmol/g functionality) were purchased from Aldrich and used as received. Hydrobromic acid in glacial acetic acid (HBr/AcOH, 450 g/L) were purchased from Alfa Aesar and used without further purification. Fetal bovine serum (FBS), penicillin, streptomycin, and Dulbecco's modified Eagle's medium (DMEM) were purchased from GIBCO and used as received. Ethidium bromide, 3-[4,5-dimethylthiazol-2-yl]-2,5-diphenyltetrazolium bromide (MTT), and branched polyethylenimine

(PEI, M_w = 25000) were purchased from Aldrich and used as received. Green fluorescent protein (GFP) expressing pDNA and luciferase expressing pDNA (Luc) were purchased from Aldevron and used as received. Tetrahydrofuran (THF) and toluene were refluxed over sodium/benzophenone and distilled prior to use. Trifluoroacetic acid (TFA) and all other chemicals were purchased from Sinopharm Chemical Reagent Co. Ltd. and used as received. ε-Benzyloxycarbonyl-*L*-lysine *N*-carboxyanhydride (ZLL-NCA)[49], 3,5-bis(propargyloxy)-benzyl alcohol (BPBA)[50], alkynyl- functionalized Wang resin[31], 3-azidopropylamine[51], and azido-terminated PEO (PEO_{113}-N_3)[52] were synthesized according to established literature procedures.

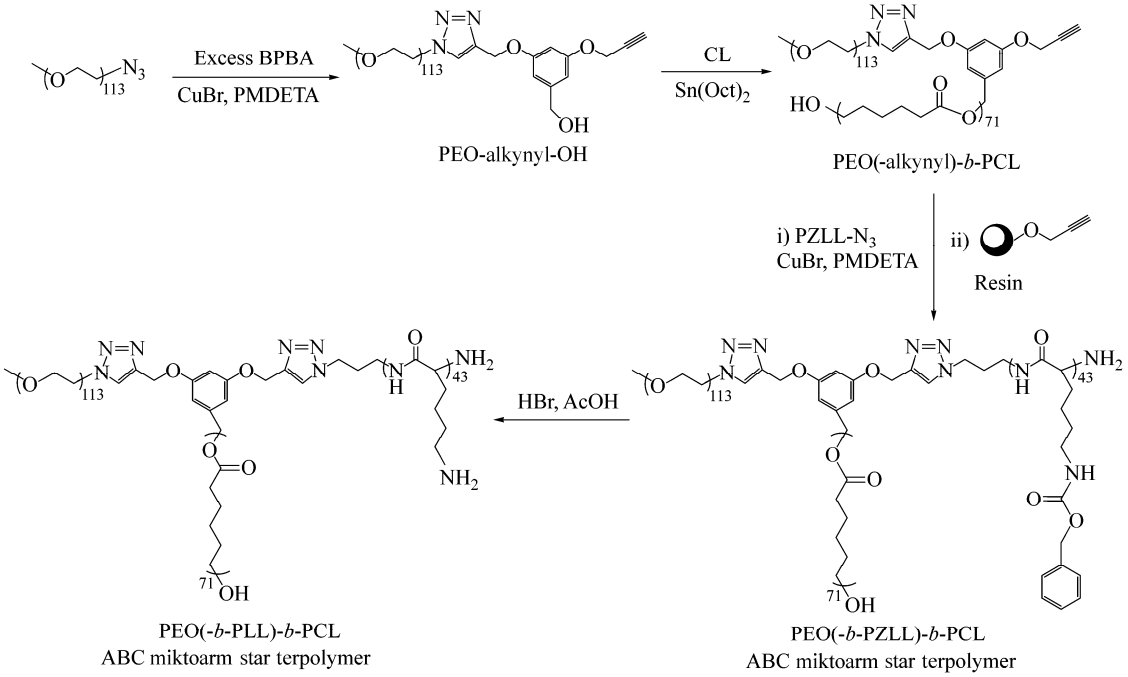

Scheme 2 Schematic illustrations for the synthesis of ABC-type miktoarm star polypeptide hybrid copolymers, PEO(-*b*-PLL)-*b*-PCL, *via* the combination of ROP and consecutive click reactions

Sample Preparation

General approaches employed to the synthesis of PEO-alkynyl-OH, PEO(-alkynyl)-*b*-PCL diblock copolymer, and ABC-type miktoarm star polypeptide hybrid copolymers, PEO(-*b*-PZLL)-*b*-PCL and PEO(-*b*-PLL)-*b*-PCL, are shown in Scheme 2.

Synthesis PEO-alkynyl-OH

Into a 30 mL Schlenk tube equipped with a magnetic stirring bar, PEO_{113}-N_3 (1.51 g, 0.3 mmol), BPBA (3.24 g, 15.0 mmol), PMDETA (0.65 g, 3.75 mmol), and 15 mL dry DMF were added. After one brief freeze-thaw cycle, CuBr (0.54 g, 3.75 mmol) was introduced under protection of N_2 flow. The reaction tube was carefully degassed by three freeze-pump-thaw cycles, sealed under vacuum, and placed in an oil bath thermostated at 80 °C. After stirring for 1.5 h, the mixture was exposed to air, diluted with THF, and passed through a basic alumina column to remove copper catalysts. After removing the solvents, the residues were dissolved in THF and precipitated into an excess of diethyl ether. The above dissolution-precipitation cycle was repeated for three times. After drying in a vacuum oven overnight at room temperature, PEO_{113}-alkynyl-OH was obtained as a white solid (1.34 g, yield 85%; $M_{n,GPC}$ = 4.8 kDa, M_w/M_n = 1.06).

Synthesis of PEO(-alkynyl)-b-PCL block copolymer by ROP of ε-CL

PEO(-alkynyl)-*b*-PCL with an alkynyl moiety at the diblock junction was prepared *via* the ROP of ε-CL monomer using $Sn(Oct)_2$ as the catalyst. To a previously flamed dried Schlenk tube equipped with a magnetic stirring bar, PEO_{113}-alkynyl-OH (0.26 g, 0.05 mmol), ε-CL (0.42 g, 3.65 mmol), $Sn(Oct)_2$ (0.2 mL, 20 g/L

solution in dry toluene, 0.01 mmol), and dry toluene (2.0 mL) were added. The reaction tube was carefully degassed by three freeze-pump-thaw cycles, sealed under vacuum, and placed in an oil bath thermostated at 90 °C. After 24 h, the reaction mixture was diluted with THF and precipitated into an excess of *n*-hexane. After filtration, the above dissolution-precipitation cycle was repeated three times. After drying in a vacuum oven overnight at room temperature, PEO(-alkynyl)-*b*-PCL was obtained as a white powder (0.58 g, yield 85%; $M_{n,GPC}$ = 13.4 kDa, M_w/M_n = 1.10). The actual DP of PCL block was calculated to be 71 based on ^{1}H-NMR analysis. Thus, the obtained diblock copolymer was denoted as PEO_{113}(-alkynyl)-*b*-PCL_{71}.

Synthesis of azido-terminated PZLL (PZLL-N_3)

Typical procedures employed for the synthesis of PZLL-N_3 are as follows. 3-Azidopropylamine (10 mg, 0.1 mmol) was dissolved in 10 mL dry DMF in a 50 mL baked flask. Freshly prepared ZLL-NCA (1.38 g, 4.5 mmol) was dissolved in 5 mL anhydrous DMF in a separate flask, and the mixture was then cannulated into 3-azidopropylamine/DMF solution *via* a double-tipped stainless needle. The reaction mixture was allowed to stir for 3 days at room temperature under dry N_2 atmosphere. After partially removing the solvents, the reaction mixture was precipitated into an excess of anhydrous diethyl ether. This purification cycle was repeated for three times. The obtained white solids were dried in a vacuum oven overnight at room temperature (1.2 g, 86% yield; $M_{n,GPC}$ = 9.9 kDa, M_w/M_n = 1.15). The actual DP of PZLL was calculated to be 43 based on ^{1}H-NMR analysis in $CDCl_3$ (containing *ca*. 10 vol% TFA). Thus, the obtained diblock copolymer was denoted as $PZLL_{43}$-N_3. Following similar procedures, $PZLL_{78}$-N_3 ($M_{n,GPC}$ = 17.6 kDa, M_w/M_n = 1.14) was also synthesized.

Synthesis of PEO(-b-PZLL)-b-PCL ABC-type miktoarm star copolymer

The synthesis of PEO(-*b*-PZLL)-*b*-PCL miktoarm star copolymers was accomplished by the click coupling of PEO_{113}(-alkynyl)-*b*-PCL_{71} precursor with $PZLL_{43}$-N_3 or $PZLL_{78}$-N_3 using CuBr/PMDETA as the catalyst, and typical procedures are as follows. The mixture of PEO_{113}(-alkynyl)-*b*-PCL_{71} (0.267 g, 0.02 mmol), $PZLL_{43}$-N_3 (0.457 g, 0.04 mmol), PMDETA (4 mg, 0.02 mmol), and DMF (10 mL) was subjected to one brief freeze-pump-thaw cycle, CuBr (3 mg, 0.02 mmol) was introduced under the protection of N_2 flow. The reaction tube was then carefully degassed by three freeze-pump-thaw cycles and placed in an oil bath thermostated at 60 °C. After 12 h, alkynyl-functionalized Wang resin (0.4 g, 0.588 mmol alkynyl groups) was added. The suspension was stirred for another 6 h at 60 °C under N_2 atmosphere. After diluting with THF and passing through a neutral alumina column to remove copper catalysts and resin, the eluents were evaporated to dryness. The residues were dissolved in THF and precipitated into an excess of *n*-hexane. The above dissolution-precipitation cycle was repeated for three times. After drying in a vacuum oven overnight at room temperature, the ABC miktoarm star polypeptide hybrid copolymer, PEO_{113}(-*b*-$PZLL_{43}$)-*b*-PCL_{71}, was obtained as a white solid (0.42 g, yield 85%; $M_{n,GPC}$ = 15.5 kDa, M_w/M_n = 1.15). Following similar procedures, PEO_{113}(-*b*-$PZLL_{78}$)-*b*-PCL_{71} miktoarm star copolymer ($M_{n,GPC}$ = 22.3 kDa, M_w/M_n = 1.13) was also synthesized.

Synthesis of PEO(-b-PLL)-b-PCL amphiphilic ABC miktoarm star copolymers

The removal of protecting benzyloxycarbonyl moieties of PEO_{113}(-*b*-$PZLL_{43}$)-*b*-PCL_{71} and PEO_{113}(-*b*-$PZLL_{78}$)-*b*-PCL_{71} finally afford the target ABC miktoarm star copolymers, and typical procedures are as follows. PEO_{113}(-*b*-$PZLL_{43}$)-*b*-PCL_{71} (0.248 g, 0.01 mmol) was dissolved in 5 mL TFA under stirring. HBr/AcOH (0.9 mL, 5 mmol HBr) was then introduced dropwise. After stirring for 30 min at room temperature, the solvents were removed under reduced pressure. The obtained solids were redispersed in water, and the dispersion was dialyzed (MW cutoff, 3.5 kDa) against deionized water for 24 h with frequent replacement of fresh water. After freeze-drying, PEO_{113}(-*b*-PLL_{43})-*b*-PCL_{71} was obtained as a white powder (0.14 g, 74% yield).

Preparation of blank and drug-loaded PEO(-b-PLL)-b-PCL micelles

In a typical example, 50 mg PEO_{113}(-*b*-PLL_{43})-*b*-PCL_{71} was added into 10 mL deionized water. After ultrasonication for 30 min, the dispersion was thermostated at 50 °C for 3 h under stirring. After further stirring at room temperature for 3 days, the obtained aqueous dispersion exhibited characteristic bluish tinge, indicating the presence of colloidal aggregates. The pH of the solution was further adjusted by the addition of NaOH or

HCl. The loading of a model chemotherapeutic drug, paclitaxel, was following similar procedures as described above except that a mixture of 50 mg PEO_{113}(-*b*-PLL_{43})-*b*-PCL_{71} and 5 mg paclitaxel were used.

In vitro Drug Release Profile Measurements

Typically, 2.5 mL paclitaxel-loaded micellar solution (1.0 g/L) of PEO_{113}(-*b*-PLL_{43})-*b*-PCL_{71} in phosphate buffer solution (PBS; 0.01 mol/L, pH 7.4) was placed in a dialysis tube (cellulose membrane; molecular weight cutoff, MWCO, is 3500 Da) and then immersed into 250 mL of PBS medium under gentle stirring at 37 °C. Periodically, 15 mL external buffer solution was removed and replaced with equal volume of fresh medium. Upon each sampling, the 15 mL buffer solution was lyophilized and the paclitaxel content was quantified by HPLC measurements. Each experiment was done in quadruple and the data are shown as the mean value plus a standard deviation (±SD).

In vitro Cytotoxicity Assay

HeLa cells were employed for *in vitro* cytotoxicity evaluation *via* the MTT assay. HeLa cells were first cultured in Dulbecco's modified Eagle medium (DMEM) supplemented with 10% fetal bovine serum (FBS), penicillin (100 units/mL), and streptomycin (100 μg/mL) at 37 °C in a CO_2/air (5:95) incubator for 2 days. For cytotoxicity assay, HeLa cells were seeded in a 96-well plate at an initial density of *ca*. 5000 cells/well in 100 μL of complete DMEM medium. After incubating for 24 h, DMEM was replaced with fresh medium, and the cells were treated with blank or drug-loaded micellar solution at varying concentrations. The treated cells were incubated in a humidified environment with 5% CO_2 at 37 °C for 48 h. The MTT reagent (in 20 μL PBS, 5 mg/mL) was added to each well. The cells were further incubated for 4 h at 37 °C. The medium in each well was then removed and replaced by 150 μL DMSO. The plate was gently agitated for 15 min before the absorbance at 570 nm was recorded by a microplate reader (Thermo Fisher). Each experiment was done in quadruple and the data are shown as the mean value plus a standard deviation (±SD).

Gel Retardation Assay

The pDNA binding ability of PEO(-*b*-PLL)-*b*-PCL micelles was evaluated by agarose gel electrophoresis. The electrostatic polyplexes were prepared at varying N/P ratios. Electrophoresis was carried out on 1% agarose gel with a current of 100 V for 10 min in TAE buffer solution (40 mmol/L Tris-HCl, 1 vol% acetic acid, and 1 mmol/L EDTA). The retardation of electrostatic complexes was visualized by staining with ethidium bromide. The final pDNA concentration is 0.4 μg per well.

In vitro Transfection and Gene Expression

HeLa cells were seeded at a density of 5×10^3 cells/well in DMEM media supplemented with 10% FBS in 96-well plates and cultured for 24 h. Before adding pDNA/micelles polyplexes, the serum-containing culture medium was replaced with 100 μL serum-free medium. pDNA/micelles polyplexes at varying N/P ratios were then added to reach a content of 200 ng DNA/well and the mixture was incubated for 4 h at 37 °C. The culture medium was then replaced with 200 μL of fresh complete medium and the cells were incubated for an additional 48 h. Transfection experiments were performed in triplicate. After incubation, the medium was removed and the cells were rinsed once with PBS. The cells in each well were treated with 200 μL of cell lysis buffer followed by freeze-thaw cycles three times to ensure complete lysis. The cell lysate was transferred into a 200 μL vial and centrifuged for 5 min at 12000 r/min and the supernatant was collected for luminescence measurements. Following the manufacturer's protocol for luciferase assay, relative luminescence units (RLU) were evaluated by Thermo Fisher microplate reader. Protein contents were quantified using BCA protein assay kit (Pierce, USA). Gene transfection efficiency is presented as RLU/mg protein.

Characterization

Molecular weights and molecular weight distributions were determined by gel permeation chromatography (GPC) equipped with Waters 1515 pump and Waters 2414 differential refractive index detector (set at 30 °C). It used a series of three linear Styragel columns HT2, HT4, and HT5 at an oven temperature of 45 °C. The eluent was DMF at a flow rate of 1.0 mL/min. A series of low polydispersity polystryene (PS) standards were

employed for the GPC calibration. All ^{1}H-NMR spectra were recorded at 25 °C on a Bruker AV300 NMR spectrometer (resonance frequency of 300 MHz for ^{1}H-NMR) operated in the Fourier transform mode. $CDCl_3$ and DMSO-d_6 were used as the solvent. Fourier transform infrared (FT-IR) spectra were recorded on a Bruker VECTOR-22 IR spectrometer. The spectra were collected at 64 scans with a spectral resolution of 4 cm^{-1}. A commercial spectrometer (ALV/DLS/SLS-5022F) equipped with a multi-tau digital time correlator (ALV5000) and a cylindrical 22 mW UNIPHASE He-Ne laser (λ_0 = 632 nm) as the light source was employed for DLS measurements. Scattered light was collected at a fixed angle of 90° for duration of *ca*. 5 min. Distribution averages and particle size distributions were computed using cumulants analysis and CONTIN routines. All data were averaged over three measurements. TEM observations were conducted on a Philips CM 120 electron microscope at an acceleration voltage of 100 kV. Samples for TEM observations were prepared by placing 10 μL micelle solution at a concentration of 0.3 g/L on copper grids, which were successively coated with thin films of Formvar and carbon. No staining procedure was conducted. Fluorescence images of transfected HeLa cells were acquired on an Olympus inverted fluorescence microscopy.

RESULTS AND DISCUSSION

Synthesis and Characterization of ABC-type Miktoarm Star Polypeptide Hybrid Copolymers

In the past decade, the integration of highly efficient click reactions with polymer chemistry has rendered the facile synthesis of polymers with controlled chemical structures, chain topologies, properties, and novel functions[53–55]. In the context of polypeptide hybrid block copolymers, Lecommandoux *et al*.[56, 57] and He *et al*.[58] synthesized poly(*γ*-benzyl-*L*-glutamate)-*b*-poly(2-(dimethylamino)ethyl methacrylate), PBLG-*b*-PDMA, and PEO-*b*-PS-*b*-PBLG linear triblock copolymers, respectively. Previously, we also synthesized AB_2 Y-shaped star polypeptide copolymers, PLL-*b*-$(PLGA)_2$, by combining ROP and click reaction techniques[31].

In the current work, we aim to synthesize biocompatible/biodegradable ABC miktoarm star polypeptide hybrid copolymers, PEO(-*b*-PLL)-*b*-PCL, *via* a combination of ROP and consecutive click reactions. General approaches employed for the synthesis of PEO(-*b*-PLL)-*b*-PCL are shown in Scheme 2. First, difunctional PEO bearing an alkynyl and a primary hydroxyl moiety at the chain end, PEO-alkynyl-OH, was prepared by the click reaction of azido-terminated PEO with an excess of 3,5-bis(propargyloxy)benzyl alcohol (BPBA). PEO(-alkynyl)-*b*-PCL diblock copolymer bearing an alkynyl moiety at the diblock junction was prepared by the ROP of *ε*-CL using PEO-alkynyl-OH as the macroinitiator and $Sn(Oct)_2$ as catalyst. Subsequently, ABC miktoarm star copolymer precursor, PEO(-*b*-PZLL)-*b*-PCL, was synthesized by reacting PEO(-alkynyl)-*b*-PCL with an excess of azido-terminated PZLL (PZLL-N_3) under click reaction conditions. The excess PZLL-N_3 was facilely removed by "clicking" onto alkynyl-functionalized Wang resin. Finally, after hydrolysis of protecting benzyloxycarbonyl groups, the target ABC miktoarm star polypeptide hybrid copolymers, PEO(-*b*-PLL)-*b*-PCL, were obtained.

The click reaction of PEO_{113}-N_3 with BPBA in DMF at 80 °C using CuBr/PMDETA as catalysts afforded difunctional PEO_{113}-alkynyl-OH bearing one alkynyl and one primary hydroxyl functionality at the chain terminal. An excess of BPBA was used to ensure that only one propargyl group in BPBA participated in the click reaction with PEO_{113}-N_3. ^{1}H-NMR spectrum of PEO_{113}-alkynyl-OH and the corresponding peak assignments are shown in Fig. S1(B). The resonance signal at δ = 3.6 (peak b) can be ascribed to methylene protons of PEO. Compared to the ^{1}H-NMR spectrum of BPBA (Fig. S1A), we can clearly observe the appearance of new peaks at δ = 7.98 and 5.24 (peaks e and f), which are ascribed to proton in 1,2,3-triazole ring and triazole-C$\underline{H_2}$OPh protons, respectively. By comparing integration areas of peak f to that of peak b, the degree of end group functionalization was calculated to be nearly quantitative. Compared to that of PEO_{113}-N_3, FT-IR spectrum of PEO_{113}-alkynyl-OH indicated the complete disappearance of characteristic azide absorbance peak at 2105 cm^{-1} (Fig. S2). GPC elution peak of PEO_{113}-alkynyl-OH (Fig. S3) revealed a slight but discernible shift to the higher MW side compared to that of PEO_{113}-N_3 precursor.

PEO(-alkynyl)-*b*-PCL with one alkynyl moiety at the diblock junction was obtained by the ROP of ε-CL in toluene at 90 °C using PEO_{113}-alkynyl-OH as the initiator and $Sn(Oct)_2$ as catalyst. ^{1}H-NMR spectrum of PEO(-alkynyl)-*b*-PCL is shown in Fig. S1(C), together with the peak assignments. Compared to that of PEO-alkynyl-OH (Fig. S1B), the ^{1}H-NMR spectrum of PEO(-alkynyl)-*b*-PCL revealed the presence of resonance signals characteristic of both PEO and PCL segments. The DP of PCL block was calculated to be 71 from ^{1}H-NMR analysis. Thus, the obtained diblock copolymer was denoted as PEO_{113}(-alkynyl)-*b*-PCL_{71}. Figure S2 shows FT-IR spectrum of PEO_{113}(-alkynyl)-*b*-PCL_{71}, clearly revealing the presence of a new absorption band at 1731 cm^{-1}, which is characteristic of carbonyl moieties in PCL block. Compared to that of PEO_{113}-alkynyl-OH (Fig. S3), the elution peak of PEO_{113}(-alkynyl)-*b*-PCL_{71} clearly shifted to the higher MW side. This indicated a complete consumption of PEO_{113}-alkynyl-OH macroinitiator. GPC analysis gave an M_n of 13.4 kDa and an M_w/M_n of 1.10 for PEO_{113}(-alkynyl)-*b*-PCL_{71}.

The next three steps involved in the preparation of ABC-type miktoarm star copolymers, PEO(-*b*-PLL)-*b*-PCL, were the synthesis of azido-terminated PZLL (PZLL-N_3), the click reaction of PEO(-alkynyl)-*b*-PCL with PZLL-N_3, and the final deprotection step (Scheme 2). 3-Azidopropylamine was used as an initiator for the ROP of ZLL-NCA, leading to the formation of PZLL-N_3. GPC analysis of PZLL-N_3 in DMF revealed a monomodal and symmetric peak (Fig. S3c), giving an M_n of 9.9 kDa and an M_w/M_n of 1.15. The actual DP of PZLL was determined to be 43 by ^{1}H-NMR analysis in $CDCl_3$ (containing *ca*. 10 vol% TFA). Moreover, FT-IR spectrum of $PZLL_{43}$-N_3 clearly revealed the presence of absorbance peak at *ca*. 2096 cm^{-1} (Fig. S2), which is characteristic of the terminal azide group in $PZLL_{43}$-N_3.

The click reaction of PEO_{113}(-alkynyl)-*b*-PCL_{71} with $PZLL_{43}$-N_3 afforded PEO_{113}(-*b*-$PZLL_{43}$)-*b*-PCL_{71} (Scheme 2). During the click reaction, excess PZLL-N_3 was used to ensure the complete consumption of PEO_{113}(-alkynyl)-*b*-PCL_{71}. It is worthy of noting that unreacted PZLL-N_3 can be facilely removed by clicking onto alkynyl-functionalized Wang resin. The formation of well-defined ABC-type miktoarm star polypeptide hybrid copolymer was confirmed by GPC, FT-IR, and ^{1}H NMR analysis (Figs. S2–S4). Compared to those of PEO_{113}(-alkynyl)-*b*-PCL_{71} and $PZLL_{43}$-N_3, the monomodal GPC elution peak of PEO_{113}(-*b*-$PZLL_{43}$)-*b*-PCL_{71} exhibited an discernible shift to the higher MW side, giving an M_n of 15.5 kDa and an M_w/M_n of 1.15 (Fig. S3). Moreover, the absence of a shoulder peak at the lower MW side confirmed that unreacted $PZLL_{43}$-N_3 has been successfully removed *via* click coupling onto alkynyl-functionalized Wang resin and subsequent simple filtration. Figure S2 shows the FT-IR spectrum of PEO_{113}(-*b*-$PZLL_{43}$)-*b*-PCL_{71}. Compared to those of $PZLL_{43}$-N_3 and PEO_{113}(-alkynyl)-*b*-PCL_{71}, we can observe the disappearance of characteristic azide absorbance peak at *ca*. 2096 cm^{-1}. Figure S4(A) shows ^{1}H-NMR spectrum of PEO_{113}(-*b*-$PZLL_{43}$)-*b*-PCL_{71}, which revealed all characteristic signals of PEO, PCL, and PZLL. Most importantly, relative chain length ratios between PEO, PZLL, and PCL arms derived from the integral ratios of peaks a, l, and e agreed quite well with the desired chemical structure of PEO_{113}(-*b*-$PZLL_{43}$)-*b*-PCL_{71}.

The obtained PEO(-*b*-PZLL)-*b*-PCL ABC-type miktoarm star copolymer was then subjected to hydrolysis to remove benzyloxycarbonyl protecting groups to afford the target PEO(-*b*-PLL)-*b*-PCL. Figure S4(B) shows a typical ^{1}H-NMR spectrum of the hydrolysis product, PEO_{113}(-*b*-PLL_{43})-*b*-PCL_{71}, in DMSO-d_6. Compared to that of PEO_{113}(-*b*-$PZLL_{43}$)-*b*-PCL_{71} precursor in $CDCl_3$ (Fig. S4A), resonance signals characteristic of benzyloxycarbonyl groups of PZLL at δ = 7.3 and 5.0 (peaks m and l) completely disappeared, indicating the complete removal of benzyloxycarbonyl moieties.

***In vitro* Drug Release and Cell Viability Evaluation of Drug-loaded PEO(-b-PLL)-b-PCL Micelles**

Figure 1(a) shows hydrodynamic radius distribution, $f(R_h)$, of PEO_{113}(-*b*-PLL_{43})-*b*-PCL_{71} micelles in aqueous solution at pH 7.4, R_h of micellar nanoparticles ranges from 15 nm to 55 nm with an intensity-average hydrodynamic radius, $<R_h>$, of *ca*. 31 nm and a polydispersity index, μ_2/Γ^2, of 0.08. TEM measurements were then employed to investigate the morphology of PEO_{113}(-*b*-PLL_{43})-*b*-PCL_{71} micelles, revealing the presence of relatively uniform spherical nanoparticles with diameters in the range of 20–40 nm (Fig. 1b). It is well-known that the TEM technique determines nanoparticle dimensions in the dry state, whereas dynamic LLS reports

intensity-average dimensions in solution, thus, size dimensions of micelles measured by TEM and DLS techniques agrees reasonably well with each other.

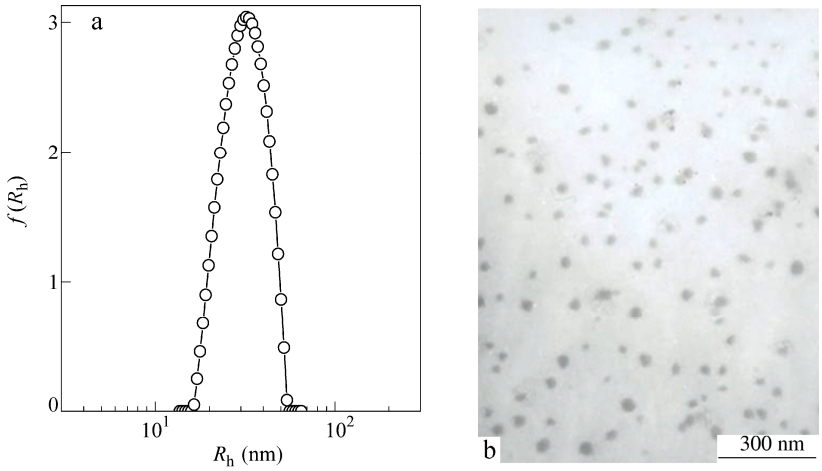

Fig. 1 (a) Typical hydrodynamic radius distribution, $f(R_h)$, recorded for the aqueous dispersion of PEO_{113}(-*b*-PLL_{43})-*b*-PCL_{71} micelles; (b) Typical TEM image obtained by drying the aqueous dispersion of PEO_{113}(-*b*-PLL_{43})-*b*-PCL_{71} micelles on copper grid

Hydrophobic cores of PEO_{113}(-*b*-PLL_{43})-*b*-PCL_{71} micellar nanoparticles were then employed to encapsulate a model hydrophobic anticancer drug, paclitaxel. The drug loading content was determined to be *ca*. 5.0 wt% relative to the amount of polymeric micelles. *In vitro* drug release profile of paclitaxel-loaded PEO_{113}(-*b*-PLL_{43})-*b*-PCL_{71} micelles was measured under simulated physiological condition (PBS buffer, pH 7.4, 37 °C). As shown in Fig. 2(a), relatively fast release of encapsulated paclitaxel was observed for the first 3 h. At extended time periods, the release rate slowed down and the cumulative drug release reaches *ca*. 65% after 60 h.

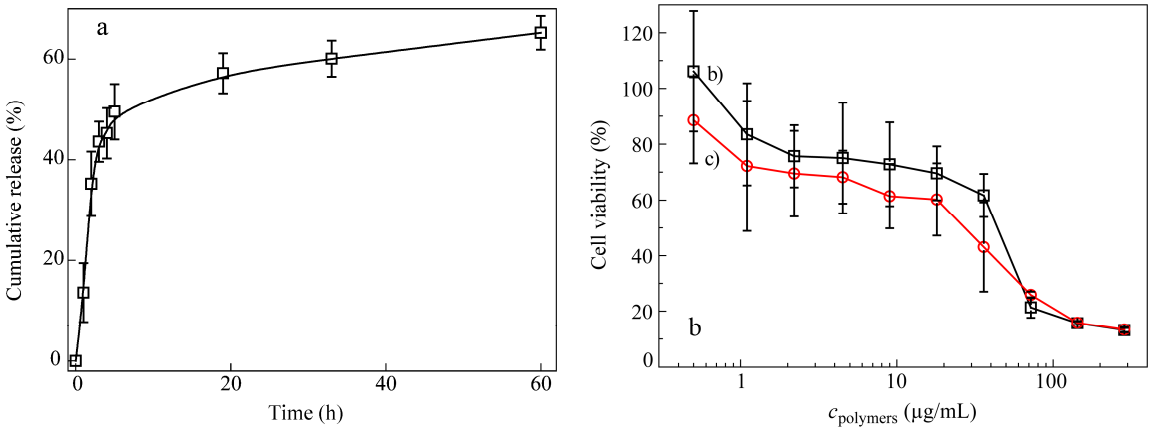

Fig. 2 (a) *In vitro* drug release profile of paclitaxel from drug-loaded PEO_{113}(-*b*-PLL_{43})-*b*-PCL_{71} micelles at 37 °C (phosphate buffer, pH 7.4). Determination of cytotoxicity *via* MTT assays of HeLa cells after incubating with (b) blank and (c) paclitaxel-loaded PEO_{113}(-*b*-PLL_{43})-*b*-PCL_{71} micelles at varying concentrations
Data points are presented as the mean ±SD of quadruple measurements.

HeLa cells were employed to evaluate the *in vitro* anticancer efficacy of the nanocarriers. As shown in Fig. 2(b), blank PEO_{113}(-*b*-PLL_{43})-*b*-PCL_{71} micelles already exhibited cytotoxicity to some extent, primarily due to the presence of cationic PLL segments within micellar coronas. At a polymer concentration of 36 μg/mL,

ca. 61% cells still remained alive. However, substantial cell death can be observed by treating HeLa cells with PEO_{113}(-*b*-PLL_{43})-*b*-PCL_{71} micelles at even higher concentrations. Compared to that of blank micelles, paclitaxel-loaded ones led to further decreased cell viability and *ca*. 43% of HeLa cells remains alive at a micellar concentration of 36 μg/mL, for which the loaded paclitaxel concentration is *ca*.1.8 μg/mL (Fig. 2c). From Fig. 2, we can also tell that at polymer concentrations higher than *ca.* 70 μg/mL, both blank and paclitaxel-loaded PEO_{113}(-*b*-PLL_{43})-*b*-PCL_{71} micelles exhibited prominent cytotoxicity, with the cell viability being less than 25%.

Characterization of PEO(-b-PLL)-b-PCL Micelles/pDNA Polyplexes and Co-delivery of Drug and Plasmid DNA

Due to that hydrophilic coronas of PEO(-*b*-PLL)-*b*-PCL micelles contain positively charged PLL polypeptide segments, they are also capable of forming electrostatic polyplexes with negatively charged pDNA and act as DNA delivery vehicles (Scheme 1)[37, 38]. Moreover, the co-delivery of hydrophobic drugs and pDNA should also be possible by utilizing hydrophobic micellar cores[59, 60] and positively charged coronas, respectively. Previous literature reports have already verified that the strategy of drug and gene co-delivery by the same nanocarrier can exhibit synergistic therapeutic effects in some specific cases[46, 61]. For example, Bae *et al*.[47]. and Zhong *et al*.[61] fabricated two different cationic micelles of block copolymers as co-delivery vehicles of hydrophobic drugs and pDNA/siRNA.

Inspired by these examples, we attempted to investigate the potential of PEO_{113}(-*b*- PLL_{43})-*b*-PCL_{71} micellar nanoparticles as co-delivery vehicles. Gel retardation assay was used to investigate pDNA binding affinity of blank and drug-loaded PEO_{113}(-*b*-PLL_{43})-*b*-PCL_{71} micelles. As shown in Fig. 3(a), due to the presence of cationic nature of PLL segments within micellar coronas, PEO_{113}(-*b*-PLL_{43})-*b*-PCL_{71} micelles can effectively form electrostatic complexes with pDNA at N/P ratios higher than *ca*. 2. In addition, paclitaxel-loaded PEO_{113}(-*b*-PLL_{43})-*b*-PCL_{71} micelles exhibit complexation capabilities comparable to that of blank micelles (Fig. 3b). This is reasonable considering that the hydrophobic drug is encapsulated within micellar cores, whereas the complexation between micelles and pDNA only involves positively charged micellar coronas. DLS and zeta potential experiments were also conducted for pDNA/micelles polyplexes. As shown in Fig. S5, with the increase of N/P ratios from 0.5 to 32, the $<D_h>$ of polyplexes formed between pDNA with blank or paclitaxel-loaded PEO_{113}(-*b*-PLL_{43})-*b*-PCL_{71} micelles decreased considerably at low N/P ratios and then stabilized out; at a N/P ratio of 32, the average hydrodynamic diameters were *ca.* 280 and 260 nm, respectively. Concomitantly, the zeta potential of polyplexes increased substantially in the N/P ratio range of 0.5–32 and finally reached +37 and +40 mV at N/P ratio of 32. In agreement with that of gel retardation assay results, we can also tell that the zeta potential of polyplexes actually changed from negative to positive at a critical N/P ratio of *ca.* 2. However, the continuous increase of zeta potential above this critical value also implied that further structural arrangement of micellar polyplexes occurred.

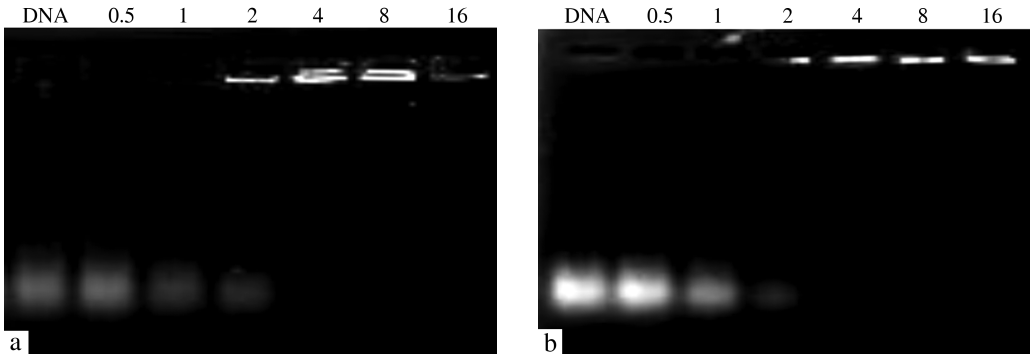

Fig. 3 Gel electrophoresis analysis of pDNA mobility upon forming electrostatic complexes with (a) blank and (b) paclitaxel-loaded PEO_{113}(-*b*-PLL_{43})-*b*-PCL_{71} micelles at varying N/P ratios

In vitro cell transfection experiments were further conducted on HeLa cells by using GFP expressing pDNA under serum-free conditions and PEI 25 K was used as control. As shown in Fig. 4, polyplexes of PEO_{113}(-*b*-PLL_{43})-*b*-PCL_{71} micelles/pDNA at N/P ratios of 4, 8, and 16 exhibited relatively lower transfection efficiency in comparison with that of PEI 25 K at an optimum N/P ratio of 10, which reasonably agreed with relevant literature reports concerning the low transfection efficiency of PLL homopolymer. However, compared to that of blank micelles, polyplexes of pDNA with paclitaxel-loaded PEO_{113}(-*b*-PLL_{43})-*b*-PCL_{71} micelles exhibited slightly improved transfection efficiency. This is probably due to the anti-mitotic feature of paclitaxel, thus leading to more pDNA entering into cell nuclei[46].

Previously, Wu *et al.*[62] reported that free polycations might play a vital role for the effective *in vitro* gene transfection. Inspired by this, polyplexes of PEO_{113}(-*b*-PLL_{43})-*b*-PCL_{71}/pDNA at a N/P ratio of 4 were prepared at first, and then additional free PEI 25 K was added to reach a final N/P ratio of 10. As shown in Fig. 5, *in vitro* transfection experiments revealed that considerably enhanced transfection efficiency can be achieved, although still lower than that exhibited by polyplexes of pDNA/PEI 25 K. This implies that the chemical structures and topologies of polycations, *i.e.*, excess PEO_{113}(-*b*-PLL_{43})-*b*-PCL_{71} micelles versus excess PEI, also plays an indispensible role during pDNA transfection.

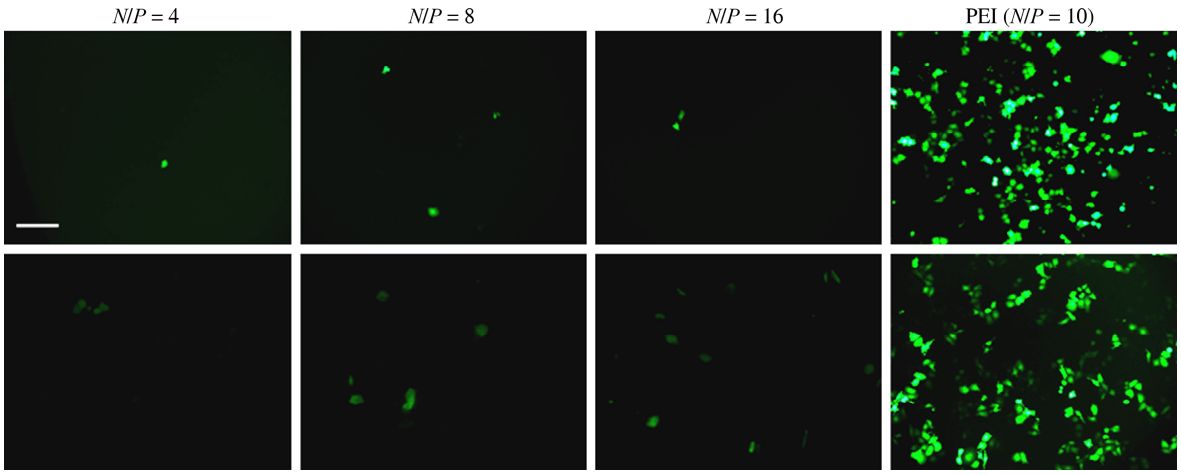

Fig. 4 Fluorescence images of HeLa cells transfected by polyplexes of GFP plasmid with (top panel) blank and (bottom panel) paclitaxel-loaded PEO_{113}(-*b*-PLL_{43})-*b*-PCL_{71} micelles at N/P ratios ranging from 4 to 16. Cell transfection images of PEI_{25k}/GFP plasmid polyplexes at an optimum N/P ratio of 10 were used as a positive control. Scale bar represents 50 μm.

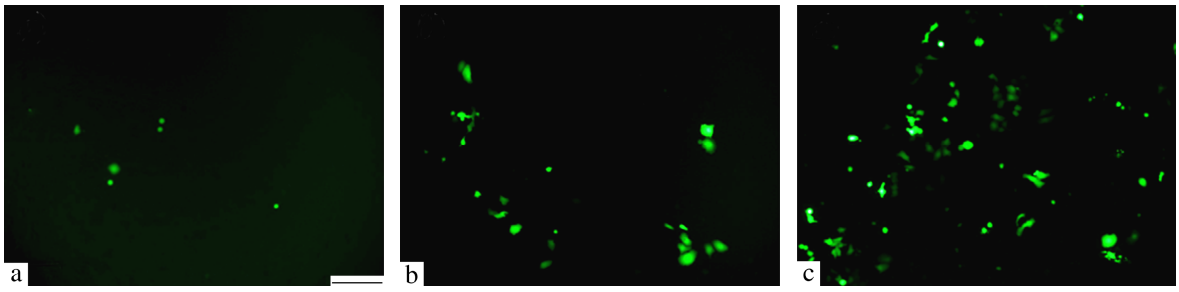

Fig. 5 Fluorescence images of HeLa cells transfected by the polyplexes of GFP plasmid with (a) blank and (b) paclitaxel-loaded PEO_{113}(-*b*-PLL_{43})-*b*-PCL_{71} micelles at a N/P ratio of 4; additional free PEI was added after polyplexes formation to reach a final N/P ratio of 10 in (a) and (b). (c) Cell transfection image of PEI_{25k}/GFP plasmid polyplexes at an optimum N/P ratio of 10 was used as a positive control. Scale bar represents 50 μm.

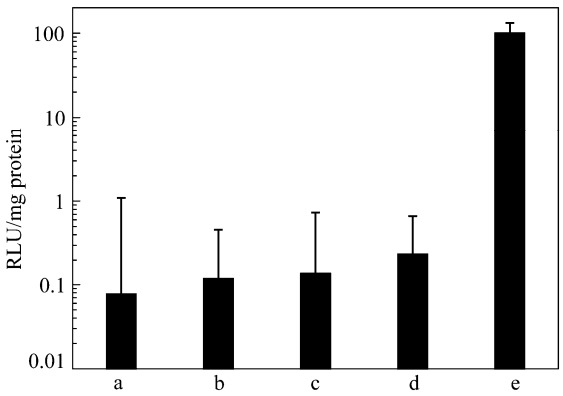

Fig. 6 Variation of *in vitro* transfection efficiencies of luciferase expressing pDNA into HeLa cells by polyplexes of plasmid DNA with (a and c) blank and (b and d) paclitaxel-loaded PEO_{113}(-*b*- PLL_{43})-*b*-PCL_{71} micelles at (a and b) N/P ratio = 8 and (c and d) N/P ratio = 4. In (c) and (d), additional free PEI was added after polyplexes formation to reach a final N/P ratio of 10. (e) Cell transfection efficiency of PEI_{25k}/GFP plasmid polyplexes at an optimum N/P ratio of 10 was used as a positive control.

Finally, quantitative assay of transfection efficiency was further conducted using luciferase expressing pDNA as the reporter gene. As shown in Fig. 6, polyplexes of pDNA with paclitaxel-loaded PEO_{113}(-*b*-PLL_{43})-*b*-PCL_{71} micelles exhibited *ca*. 53% improvement in transfection efficiency at a N/P ratio of 8 in comparison with that exhibited by pDNA/blank micelles polyplexes. In addition, by introducing free PEI into PEO_{113}(-*b*-PLL_{43})-*b*-PCL_{71}/pDNA polyplexes, further increase of pDNA transfection efficiency can be achieved.

CONCLUSIONS

In summary, we fabricated cationic micellar nanoparticles from ABC-type miktoarm star polypeptide hybrid copolymers consisting of poly(ethylene oxide), poly(L-lysine), and poly(ε-caprolactone) arms, PEO(-*b*-PLL)-*b*-PCL, and investigated their functional applications as co-delivery nanocarriers of chemotherapeutic drugs and plasmid DNA. Miktoarm star copolymer precursors, PEO(-*b*-PZLL)-*b*-PCL, were synthesized at first via the combination of consecutive "click" reactions and ring-opening polymerizations (ROP). Subsequently, the deprotection of PZLL arm afforded amphiphilic miktoarm star copolymers, PEO(-*b*-PLL)-*b*-PCL. In aqueous media at pH 7.4, PEO(-*b*-PLL)-*b*-PCL self-assembles into micelles consisting of PCL cores and hydrophilic PEO/PLL hybrid coronas. The hydrophobic micellar cores can effectively encapsulate model hydrophobic anticancer drug, paclitaxel; whereas positively charged PLL arms within mixed micellar corona are capable of forming electrostatic polyplexes with negatively charged plasmid DNA (pDNA) at N/P ratios higher than *ca.* 2. Thus, PEO(-*b*-PLL)-*b*-PCL micelles can act as co-delivery nanovehicles for both chemotherapeutic drugs and genes. Furthermore, polyplexes of pDNA with paclitaxel-loaded PEO(-*b*-PLL)-*b*-PCL micelles exhibited improved transfection efficiency compared to that of pDNA/blank micelles. We expect that the reported strategy of varying chain topologies for the fabrication of co-delivery polymeric nanocarriers can be further applied to integrate with other advantageous functions such as targeting, imaging, and diagnostics.

SUPPORTING INFORMATION Characterization data of ^{1}H-NMR, FT-IR, GPC, Size and Zeta Potentials of miktoarm star copolymers, their precursors, and their polyplexes.

REFERENCES

1 Deming, T.J., Adv. Mater., 1997, 9: 299
2 Trzcinska, R., Szweda, D., Rangelov, S., Suder, P., Silberring, J., Dworak, A. and Trzebicka, B., J. Polym. Sci., Part A Polym. Chem., 2012, 50: 3104
3 Zhu, M.Q., Xiang, L., Yang, K., Shen, L.J., Long, F., Fan, J.B., Yi, H.Q., Xiang, J. and Aldred, M.P., J. Polym. Res., 2012, 19: 9808
4 Zhang, S.S., Chen, C.Y. and Li, Z.B., Chinese J. Polym. Sci., 2013, 31(2): 201
5 Li, H.B., Tian, Z., Zhang, A.Y. and Feng, Z.G., Chinese J. Polym. Sci., 2009, 27(3): 317
6 Gebhardt, K.E., Ahn, S., Venkatachalam, G. and Savin, D.A., J. Colloid Interface Sci., 2008, 317: 70
7 Li, C.H., Ge, Z.S., Fang, J. and Liu, S.Y., Macromolecules, 2009, 42: 2916
8 Xu, X.H., Li, C.X., Li, H.P., Liu, R., Jiang, C., Wu, Y., He, B. and Gu, Z.W., Sci. Chin. Chem., 2011, 54: 326
9 Cho, C.S., Cheon, J.B., Jeong, Y.I., Kim, I.S., Kim, S.H. and Akaike, T., Macromol. Rapid Commun., 1997, 18: 361
10 Babin, J., Rodriguez-Hernandez, J., Lecommandoux, S., Klok, H.A. and Achard, M.F., Faraday Discuss., 2005, 128: 179
11 Dimitrov, I. and Schlaad, H., Chem. Commun., 2003, 2944
12 Lubbert, A., Castelletto, V., Hamley, I.W., Nuhn, H., Scholl, M., Bourdillon, L., Wandrey, C. and Klok, H.A., Langmuir, 2005, 21: 6582
13 Checot, F., Rodriguez-Hernandez, J., Gnanou, Y. and Lecommandoux, S., Polym. Adv. Technol., 2006, 17: 782
14 Schlaad, H., Smarsly, B. and Below, I., Macromolecules, 2006, 39: 4631
15 Checot, F., Rodriguez-Hernandez, J., Gnanou, Y. and Lecommandoux, S., Biomol. Eng., 2007, 24: 81
16 Gil, G.O., Losik, M., Schlaad, H., Drechsler, M. and Hellweg, T., Langmuir, 2008, 24: 12823
17 Sun, J., Chen, X.S., Deng, C., Yu, H.J., Xie, Z.G. and Jing, X.B., Langmuir, 2007, 23: 8308
18 Sun, J., Deng, C., Chen, X.S., Yu, H.J., Tian, H.Y., Sun, J.R. and Jing, X.B., Biomacromolecules, 2007, 8: 1013
19 Kricheldorf, H.R. and Hauser, K., Biomacromolecules, 2001, 2: 1110
20 Caillol, S., Lecommandoux, S., Mingotaud, A.F., Schappacher, M., Soum, A., Bryson, N. and Meyrueix, R., Macromolecules, 2003, 36: 1118
21 Rong, G.Z., Deng, M.X., Deng, C., Tang, Z.H., Piao, L.H., Chen, X.S. and Jing, X.B., Biomacromolecules, 2003, 4: 1800
22 Sun, J., Chen, X.S., Lu, T.C., Liu, S., Tian, H.Y., Guo, Z.P. and Jing, X.B., Langmuir, 2008, 24: 10099
23 Holowka, E.P., Pochan, D.J. and Deming, T.J., J. Am. Chem. Soc., 2005, 127: 12423
24 Rodriguez-Hernandez, J. and Lecommandoux, S., J. Am. Chem. Soc., 2005, 127: 2026
25 Rao, J.Y., Luo, Z.F., Ge, Z.S., Liu, H. and Liu, S.Y., Biomacromolecules, 2007, 8: 3871
26 Zhang, X.Q., Li, J.G., Li, W. and Zhang, A., Biomacromolecules, 2007, 8: 3557
27 Pitsikalis, M., Pispas, S., Mays, J.W. and Hadjichristidis, N., Adv. Polym. Sci., 1998, 135: 1
28 Babin, J., Leroy, C., Lecommandoux, S., Borsali, R., Gnanou, Y. and Taton, D., Chem. Commun., 2005, 1993
29 Abraham, S., Ha, C.S. and Kim, I., J. Polym. Sci., Part A Polym. Chem., 2006, 44: 2774
30 Babin, J., Taton, D., Brinkmann, M. and Lecommandoux, S., Macromolecules, 2008, 41: 1384
31 Rao, J.Y., Zhang, Y.F., Zhang, J.Y. and Liu, S.Y., Biomacromolecules, 2008, 9: 2586
32 Li, Z.B., Kesselman, E., Talmon, Y., Hillmyer, M.A. and Lodge, T.P., Science, 2004, 306: 98
33 Li, Z.B., Hillmyer, M.A. and Lodge, T.P., Nano Lett., 2006, 6: 1245
34 Li, Z.B., Hillmyer, M.A. and Lodge, T.P., Langmuir, 2006, 22: 9409
35 Zhang, Y.F., Liu, H., Dong, H.F., Li, C.H. and Liu, S.Y., J. Polym. Sci., Part A Polym. Chem., 2009, 47: 1636
36 Zhang, W.D., Zhang, W., Zhang, Z.B., Cheng, Z.P., Tu, Y.F., Qiu, Y.S. and Zhu, X.L., J. Polym. Sci., Part A Polym. Chem., 2010, 48: 4268
37 Du, J., Sun, Y., Shi, Q.S., Liu, P.F., Zhu, M.J., Wang, C.H., Du, L.F. and Duan, Y.R., Int. J. Mol. Sci., 2012, 13: 516
38 Zhou, D.Z., Li, C.X., Hu, Y.L., Zhou, H., Chen, J.T., Zhang, Z.P. and Guo, T.Y., J. Mater. Chem., 2012, 22: 10743
39 Mintzer, M.A. and Simanek, E.E., Chem. Rev., 2009, 109: 259
40 Meng, F.H., Hennink, W.E. and Zhong, Z., Biomaterials, 2009, 30: 2180

41 Janat-Amsbury, M.M., Yockman, J.W., Lee, M., Kern, S., Furgeson, D.Y., Bikram, M. and Kim, S.W., Mol. Ther., 2004, 9: 829
42 Yue, X.Y., Qiao, Y., Qiao, N., Guo, S.T., Xing, J.F., Deng, L.D., Xu, J.Q. and Dong, A.J., Biomacromolecules, 2010, 11: 2306
43 Lu, X., Wang, Q.Q., Xu, F.J., Tang, G.P. and Yang, W.T., Biomaterials, 2011, 32: 4849
44 Sun, T.M., Du, J.Z., Yao, Y.D., Mao, C.Q., Dou, S., Huang, S.Y., Zhang, P.Z., Leong, K.W., Song, E.W. and Wang, J., Acs Nano, 2011, 5: 1483
45 Xiong, X.B. and Lavasanifar, A., Acs Nano, 2011, 5: 5202
46 Wang, Y., Gao, S.J., Ye, W.H., Yoon, H.S. and Yang, Y.Y., Nat. Mater., 2006, 5: 791
47 Qiu, L.Y. and Bae, Y.H., Biomaterials, 2007, 28: 4132
48 Guo, S.T., Qiao, Y., Wang, W.W., He, H.Y., Deng, L.D., Xing, J.F., Xu, J.Q., Liang, X.J. and Dong, A.J., J. Mater. Chem., 2010, 20: 6935
49 Bromberg, L. and Levin, G., Bioconjugate Chem., 1998, 9: 40
50 Wu, P., Feldman, A.K., Nugent, A.K., Hawker, C.J., Scheel, A., Voit, B., Pyun, J., Frechet, J.M.J., Sharpless, K.B. and Fokin, V.V., Angew. Chem., Int. Ed., 2004, 43: 3928
51 Lewis, W.G., Magallon, F.G., Fokin, V.V. and Finn, M.G., J. Am. Chem. Soc., 2004, 126: 9152
52 Altintas, O., Hizal, G. and Tunca, U., J. Polym. Sci., Part A Polym. Chem., 2006, 44: 5699
53 Kolb, H.C., Finn, M.G. and Sharpless, K.B., Angew. Chem., Int. Ed., 2001, 40: 2004
54 Qin, A.J., Lam, J.W.Y. and Tang, B.Z., Macromolecules, 2010, 43: 8693
55 Fu, R. and Fu, G.D., Polym. Chem., 2011, 2: 465
56 Agut, W., Taton, D. and Lecommandoux, S., Macromolecules, 2007, 40: 5653
57 Agut, W., Agnaou, R., Lecommandoux, S. and Taton, D., Macromol. Rapid Commun., 2008, 29: 1147
58 Wang, K., Liang, L.Y., Lin, S.L. and He, X.H., Eur. Polym. J., 2008, 44: 3370
59 Liu, T., Qian, Y.F., Hu, X.L., Ge, Z.S. and Liu, S.Y., J. Mater. Chem., 2012, 22: 5020
60 Li, X.J., Qian, Y.F., Liu, T., Hu, X.L., Zhang, G.Y., You, Y.Z. and Liu, S.Y., Biomaterials, 2011, 32: 6595
61 Zhu, C.H., Jung, S., Luo, S.B., Meng, F.H., Zhu, X.L., Park, T.G. and Zhong, Z.Y., Biomaterials, 2010, 31: 2408
62 Yue, Y.A., Jin, F., Deng, R., Cai, J.G., Chen, Y.C., Lin, M.C.M., Kung, H.F. and Wu, C., J. Controlled Release, 2011, 155: 67